Using integrated near-surface geophysical surveys to aid mapping and interpretation of geology in an alluvial landscape within a 3D soil-geology framework.

A.M. Tye, H. Kessler, K. Ambrose, J.D.O. Williams, D. Tragheim, A. Scheib, M. Raines and O. Kuras

British Geological Survey, Keyworth, Nottingham, NG12 5GG

Corresponding author: atye@bgs.ac.uk

Abstract

An integrated geological, geophysical and remote sensing survey was undertaken as part of the construction of a high resolution 3D model of the shallow subsurface geology of part of the Trent Valley in Nottinghamshire, U.K. The 3D model was created using the GSI3D software package and geophysical techniques used included Ground Penetrating Radar (GPR), Electrical Resistivity Tomography (ERT) and Automated Resistivity Profiling (ARP). In addition, the remote sensing techniques of Light Detection and Ranging (LIDAR) and Airborne Thematic Mapping (ATM) were used. The objective of the study was to assess the contribution of these techniques to improve the geological mapping and interpretation of terrace deposits and other geological features. The study site had an area of ~2 km^2 and consisted of a Triassic mudstone escarpment, overlain first by a sand and gravel river terrace that extended to the modern floodplain of the River Trent. ARP mapping proved to be the central tool in identifying and positioning geological features at a greater resolution than would be obtained through traditional geological mapping and borehole observation. These features included (i) a buried cliff delineating the south eastern limits of the incised Trent valley, (ii) siltstone beds within the Gunthorpe Member of the Mercia Mudstone Group and (iii) the variability of the sediments within the river terrace. A long ERT transect across the site successfully imaged the buried cliff and outcropping siltstone beds on the escarpment. Combined ERT and GPR transects revealed the depth of the sand and gravel deposits (Holme Pierrepont sands and gravels), whilst the GPR provided information about the depositional environment. Remote sensing using LIDAR proved essential in the original geological survey because it confirmed the absence of a second river terrace that had been previously thought to exist. This case study demonstrates the importance of combining geophysical techniques with traditional geological survey and borehole analysis, in order to create high-resolution 3D geological models, which are increasingly being used as a platform to understand and solve environmental problems.

1. Introduction

As anthropogenic activity increases pressure on land and water resources, a greater understanding of the structure of the near surface environment or 'critical zone' is required (Brantley *et al*., 2007; Anderson *et al*., 2007). Developing a systems-based approach, rather than studying isolated components of the near surface environment, will aid the understanding of natural processes as well as anthropogenic impacts on the shallow earth surface. One advancing technology that can provide a platform for understanding such processes and impacts are digital geological models that include soils and superficial geology. These can be created using specialised software such as GSI3D (Kessler *et al*., 2009). The construction of a 3D model is based on a geoscientist's ability to interpret the geological terrain, borehole data and geophysical information at their disposal in one single virtual environment. Once complete the 3D model can be considered a predictive tool which can be interrogated at any one point to assess the spatial geological structure within the modelled area. One of the many attributes of the GSI3D software is that the model can be interrogated so that borehole logs and cross-sections of the geology can be generated at any point, thus providing an interactive interface for the user community. It also provides a spatial framework in which geological units are considered to be domains. Property information can be assigned to the domains or they can be re-classified. For example, domains can be reclassified as hydro-geological units (Macmillan *et al.*, 2000; Lelliott *et al*., 2006). Thus they can provide an important management tool, especially for non-geologists, enabling the depth and relationships of the different geological or soil domains to be seen in a spatial context. In future these models could potentially incorporate or be used as a basis for process-based numerical models. Therefore the geological and soil mapping of these models is required to be as accurate as possible.

One particular environment where 3D models of the near surface environment can have a major impact is that of river terraces. These usually consist of a series of fluvial deposits of great heterogeneity that can be important for many reasons. For example, river terraces can be a major

source of aggregates for the construction industries. One of the benefits of the GSI3D software and models are that volumes of sand and gravel deposits can be calculated by converting mapped areas into volumes (Chambers *et al*., 2008). With increasing soil sealing and building on floodplains, the utility of 3D models can help determine and model the hydrology and storage of water in terraces and flood plains. Knowledge of the volume of alluvial deposits and channels with low storage volumes in the floodplain will enable improved calculations of the water storage capacity of the terrace deposits within wider flood water storage schemes. For example, Newell (2007) determined the volume of man made deposits (low storage capacity) within a 3D model of the River Thames at Oxford as part of a project examining flood defence systems. Accurate 3D geological representation and property information are used within ground water modelling packages such as ZOOM or MODFLOW (Merritt *et al*., 2007; Hughes *et al*., 2008). The accurate positioning and knowledge of different deposits and their transmissivities are essential in understanding groundwater flow and the potential for contaminant transfer and possible areas of attenuation.

Typically, 3D models are constructed through traditional geological surveys and combined with geological borehole information. However, geophysical and remote sensing methodologies have increasingly been used to improve the understanding and interpretation of complex superficial alluvial or quaternary deposits. Subsurface imaging techniques such as Electrical Resistivity Tomography (ERT) and Ground Penetrating Radar (GPR), especially if used in combination, can be a particularly effective tool at interpreting depositional environments and features in flood plains (Hugenholtz *et al*., 2007; Lunt *et al*., 2004; Lunt and Bridge, 2004; Neal, 2004). In another example, Gourry *et al*. (2003) used three classical geophysical methods to map alluvial deposits in the middle reaches of the River Loire. These included electromagnetic profiling supplemented by electrical soundings, electrical resistivity and ground penetrating radar. The use of these techniques enabled the detection of clayey-peaty palaeochannels and the production of conductivity maps that provided a general plan view of the various alluvial deposits and palaeochannels, along with estimates of the

depth of incision of the Loire into the autochthonous calcareous rock. Greater knowledge of the fluvial system allowed an improved reconstruction of the historical river dynamics of the Loire River.

In the current study, a series of geophysical surveys were carried out to demonstrate their potential to improve the accuracy of the geological mapping within a 3D model of the near surface environment around a typical river terrace landscape adjoining the River Trent in Nottinghamshire, U.K. This landscape consisted of a Triassic mudstone escarpment that is overlain in the Trent Valley by a series of mainly sand and gravel terrace deposits. The geophysical surveys undertaken included GPR, ERT, ARP, LIDAR and ATM remote sensing data. It was hoped that the geophysical techniques used would (i) improve the identification of geological features and the spatial distribution of alluvial deposits mapped and (ii) aid interpretation of the Quaternary fluvial system of this part of the Trent valley. It was also considered important to assess the use of each survey technique for use in future surveys. A series of examples are provided demonstrating the importance of geophysical survey and remote sensing techniques in developing high resolution 3D geological models.

2. Materials and Methods

2.1 Study Area

The study area was situated around the village of Shelford, lying ~ 4 km east of the city limits of Nottingham, in the Trent valley. The area was chosen as a suitable site for developing 3D framework methodology as it is typical of a large section of the Trent valley and provides considerable variation in bedrock and superficial geology. Figure 1 shows the extent of the study area of which the 3D model formed a major part. The site extends south-eastwards from the River Trent, crossing alluvium and river terrace deposits on the low ground at 18-20 m Above Ordnance Datum (AOD), rising up an escarpment in the Mercia Mudstone Group formed by the Cotgrave Sandstone Member. The highest ground in the south-east of the site is capped by glacial till at more

than 50 m AOD. The predominant current land use on the site is arable farming with small localised areas of deciduous woodland. The site also includes evidence of cultural heritage dating back to roman times and part of the site is designated as an Ancient monument (FASTRAC., 2008).

2.2 Geological Survey

Data required to conceptualize the initial 3D geological model were obtained from a combination of geological survey data, the BGS borehole archive, newly drilled boreholes and the digging of trial pits. A geological survey was commissioned in 1988 at 1:10 000 scale, along with engineering geology and hydrogeological studies, by the Department of the Environment (DofE) (Charsley *et al*., 1990). Archived information from the DofE survey was used in this study along with a new geological survey of the site undertaken at 1:10 000 scale. This new survey allowed the most appropriate sites for the digging of trial pits and drilling of new boreholes to be selected. This enabled observations in the bedrock geology to be made based on topographic features that define the Cotgrave Sandstone and its dip slope, and the hard beds of green siltstone and sandstone within the Gunthorpe and Edwalton members. The river terraces were defined by broad flat areas adjacent to the current flood plain of the River Trent. Areas of alluvium on the river terraces were defined by slight topographic hollows and locally clayey and wetter soils. Minor augering was undertaken, mainly to prove the till at the top of the escarpment and also the nature of the head, colluvium, Trent alluvium and alluvial deposits crossing the terrace outcrops.

2.2 Borehole Information

Borehole data relating to the thickness of superficial deposits and geological units were the basis upon which the 3D geological models were created. Seven archived boreholes were used from the National Geoscience Data Centre (NGDC) at the British Geological Survey, augmented by fourteen new boreholes, drilled using a Dando Terrier 2002 drilling rig, which were positioned to fill in areas of missing data. In addition, some boreholes were taken to ground truth the geophysical surveys.

2.3 3D model generation

The 3D geological model construction software used is 'Geological Surveying and Investigation in 3D (GSI3D)'. This software uses the same principles, albeit in digital formats that geologists use to make geological maps and cross-sections (Kessler and Mathers, 2004; Smith *et al*., 2008). In summary, the software combines a Digital Terrain Model (DTM), geological surface linework and downhole borehole data in order to create regularly spaced intersecting cross-sections by correlating borehole data and the outcrop-subcrops of units. Generation of these cross-sections produces a geological fence diagram which allows for production of a solid 3D model through a mathematical interpolation of the section nodes using a bespoke Delaunay triangulation based on a quad-edge algorithm (Green and Sibson, 1978). The model is built from a series of stacked Triangulated Irregular Networks (TINs), corresponding to the top and basal surface of each geological unit in the model. The basic data formats used in a GSI3D model include a DTM loaded as standard ASCII grid file, geo-registered raster images such as topographic base maps and aerial photographs, digital borehole data (locational and lithostratigraphic), geological survey data loaded as GIS shape files and geo-registered planar images (vertical and horizontal). The backbone of the software is the Generalised Vertical Section (GVS), which contains the details of all geological units in their stratigraphical order which defines the "stack" that is calculated to make the 3D geological model. A detailed description of the software methodology is given by Kessler *et al*. (2009). Details concerning the methodology and workflow of incorporating geophysical data from Shelford in GSI3D can be found in Scheib *et al*. (2007) and Williams and Scheib (2008). Figure 2 provides an example of the workflow used to create the model.

2.4 Geophysical Techniques

Three different near-surface geophysical techniques were used at the Shelford site to aid the mapping of the distribution and morphology of shallow sub-surface features in 3D; namely ARP ERT and GPR. These methods are complementary for two main reasons. Firstly, they are sensitive to contrasts in different electrical parameters (ARP and ERT map resistivity, while GPR responds to

permittivity contrasts). Secondly, ERT and GPR can provide information on physical property distributions with depth in the form of vertical 2D cross-sections, while ARP can provide detail on the lateral distribution of resistivity in the form of horizontal maps. All techniques are quantitative in a sense that they provide a numerical value for a physical property at a location in 3D space. Their combined use in a 3D environment allows for horizontal property maps to be interpreted alongside cross-sectional profiles. The positioning of all profiles was carried out in the field using differential GPS for static measurements and real-time kinematic GPS for dynamic surveys. Figure 3 reports the positions of all the geophysical surveys undertaken.

2.4.1 Automated Resistivity Profiling (ARP)

The ARP technique (Dabas, 2009) uses a patented multi-electrode device in order to make direct current (DC) measurements of sub-surface electrical resistivity along profiles with the aim of producing horizontal property maps (Dabas and Favard, 2006; Dabas and Favard, 2007). Electrical mapping using DC resistivity methods (e.g. Panissod *et al*, 1998; Kuras *et al*., 2007) has advantages over inductive methodologies due to smaller uncertainties in sensor calibration and greater control over the depth of investigation (Dabas and Tabbagh, 2003). In this context, resistivity measures the ability of the soil to conduct an electrical current, units being in Ohm-meters (Ωm).

The ARP device employed at Shelford measures the apparent resistivity (ρ_a) for three different geometrical configurations of electrodes, whereby increasing electrode separation achieves greater depth of investigation. The ARP electrodes are wheel-mounted and thus are automatically inserted into the ground and rolled along the surface, acting as current and potential dipoles. Apparent resistivity maps can provide a proxy for the spatial variation of intrinsic soil properties such as texture, clay content, moisture, stoniness and depth to substratum (Samouelian *et al*., 2005). The towed ARP array is laid out in equatorial dipole-dipole geometry and comprises one transmitter dipole and three receiver dipoles with increasing separation. The former injects a stabilised current

into the ground, the latter measure the potential that is generated as a result. The separations between the receiver dipoles and the transmitter dipole are 0.5 m, 1 m and 2 m, respectively. The individual receiver dipole sizes (i.e. tread width of the wheels) roughly correspond to these separations (i.e. the wheel base of each transmitter–receiver dipole combination). Numerical simulations have shown that the depth of investigation of each pair of dipoles is then of the same order as the respective receiver–transmitter distance (Dabas, 2009). The typical amplitude of the current is 10 mA. Measurements can be made at typical intervals of 20 cm irrespective of towing speed (up to 30 km/h on suitable terrain). The use of real-time kinematic GPS navigation within the system enables the acquisition of spatially accurate data in real-time. This survey principle facilitates highly mobile and self-contained acquisition of data over areas of ~ 40 ha/d. Typical site coverage follows a grid of parallel survey lines in a bi-directional pattern, guided by on-board navigation. In the present study at Shelford, line spacings of 1–20 m were used, with 5 m being the preferred distance as this was found to be a reasonable compromise between required spatial resolution and survey efficiency. Data processing involved application of a 1D median filter along transect, followed by a bicubic spline interpolation on a 2.5 m regular mesh.

2.4.2 Electrical Resistivity Tomography (ERT)

ERT is a geophysical technique that produces tomographic images of the sub-surface, enabling detailed structural evaluation, and the quantification of hydraulic and geotechnical parameters that are related to electrical properties (Dahlin, 1996). Features with contrasting resistivities to those of surrounding materials may be located and characterised in terms of electrical resistivity, geometry and depth of burial. 2D ERT data were acquired on a long transect (SE-NW) perpendicular to the valley strike across the Shelford site, extending from the top of the escarpment to the modern flood plain and southern bank of the River Trent. A total distance of approximately 1992 m was covered (Figure 3), with data being collected along five individual component profiles. A further 935 m of 2D ERT profile data from a concurrent project (FASTRAC, 2008) was available for analysis. The

surveys were designed to cross the full range of superficial and underlying geology present at the site. An AGI SuperSting R8 IP resistivity meter was used together with a 64-way switch box attached to stainless steel electrodes via multicore cables. An electrode separation of 3 m was employed on five profiles in order to achieve a compromise between detailed spatial resolution and areal coverage, while a spacing of 1 m was used on one short profile in order to increase the resolution of data obtained over the alluvial channel. A robust measurement command sequence was used comprising variations of the Wenner-Schlumberger array. Res2Dinv (Loke, 2007) software was used to process the data and to produce 2D electrical resistivity inverse model sections of the sub-surface. Surface topography was accounted for during inverse modelling of the data, with the maximum depth extent of the resistivity models being ~11 m below ground level. In contrast to ARP data, which represent apparent resistivities and as such are functions of sensor geometry used to acquire the data, the vertical sections obtained with ERT represent models of bulk sub-surface resistivity. This is an intrinsic physical property that is independent of sensor geometry. For the purposes of interpretation, both types of data can be compared in an approximate fashion, however truly quantitative correlation between ERT and ARP would require inverse modelling of the ARP data and accurate localisation of the resulting inverted resistivities in 3D space (both laterally and with depth).

2.4.3 Ground Penetrating Radar (GPR)

GPR is used to investigate the sub-surface by penetration and reflection of high-frequency electromagnetic waves in the ground. Reflections are generated by changes of the complex wave number of the soil or rock medium. At frequencies normally used for GPR (> 25 MHz), these changes are dominated by relative permittivity contrasts between two media, and determine the amplitude of any reflections generated (Davis and Annan, 1989). GPR is an effective method for interpreting sub-surface alluvial deposits, however the signal is attenuated by electrically conductive substrates, and thus will not effectively penetrate deposits with high clay contents. The

GPR surveys conducted at Shelford used a Pulse Ekko IV^{TM} (low frequency) system (Sensors & Software Inc.). Measurements were made using centre frequency 100 MHz antennae at 1 m separation, orientated broadside to the survey direction and moved in steps of 0.25 m. The transmitter voltage was 1000 V, with a sampling interval of 800 ps and signal stacking of 32 times. The GPR data were processed and plotted using the standard procedures detailed in Annan (1993) and Jol, et al., (2003) using pulse EKKO IV^{TM} (version 4) software. Because of the similarities between GPR and seismic reflection many seismic reflection processing techniques can be used without modification on radar data (Young *et al*, 1995; Pipan *et al*, 1999). Initial data processing involved applying a time domain filter to each trace (dewow) to remove very low frequency components, which maybe either inductive or possibly instrumentation dynamic range limitations. An automatic time zero shift correction was applied to each radar section to compensate for time zero drift and the data filtered with spatial and time averaging filters. Sections were plotted using an automatic gain control (AGC), which attempts to equalise all signals by applying a gain which is inversely proportional to the signal strength. Hence all parts of the signal, including noise, are amplified and relative amplitude information is not preserved. Migration attempts to correctly position subsurface reflection events by removing diffractions, distortions, dip displacements and out-of-line reflections. However, in this case it was not applied as tests showed little overall improvement to reflection continuity.

A LIDAR DTM was used to correct for topography and the results plotted in section form as two-way travel time against sample position. Time-to-depth conversions are shown on the profiles by determining the electromagnetic wave propagation velocity at the sites. This velocity was determined by a Common Mid-Point (CMP) analysis (Annan and Davies, 1976) at three sites across a gravel bar (Figure 3). The average velocity was found to be 0.1 m/ns, resulting in an observable signal penetration of approximately 5 m. As the vertical resolution is equal to ¼ of a radar wavelength (Davis and Annan, 1989; Jol, 1998) the 100 MHz antenna has a resolvable layer

thickness of approximately 25 cm. Approximately 1591 m of GPR data was acquired along the main geophysical profile lines (Figure 3) in order to provide comparative results and correlation with the ERT data. A further 1408 m of GPR profiles were acquired elsewhere across the study site (Figure 3). Some of the in-fill traverses were acquired using a Sensors & Software Noggin 250 MHz system in continuous mode where ground clearance permitted (usually on short pasture grass), in order to improve line coverage and calibrate with the ARP results. GPR has been used to reconstruct past depositional environments in a variety of environmental settings. In correctly processed radar profiles, and at the resolution of a survey, primary reflections usually parallel primary depositional structure. In GPR profiling, electromagnetic waves are reflected at lithofacies boundaries due to changing water content and therefore, radar reflection patterns can often reproduce the geometry of sedimentary structures. The technique has been successful in mapping the sedimentology and stratigraphy of relict high energy glaciofluvial deposits (Fisher *et al*., 1995; Jol *et al*., 1998; Van Overmeeren, 1998; McCuaig & Ricketts, 2004). Huggenburger (1993) showed in his study on the Pleistocene braided river deposits of the Rhine that GPR offers the potential to resolve sedimentary structures and lithofacies in gravel deposits.

2.5 Remote sensing techniques

2.5.1 LIDAR

LIDAR information was obtained from a Optech Airborne Laser Terrain Mapper 2033 Lidar. It was collected from an aircraft mounted laser operating in the near infra-red (NIR) (1047nm) where backscattered intensity is in effect a record of the reflectance of earth surface materials at this wavelength. A differential GPS provided detailed 3D information on the location of the laser unit, while an inertial measurement unit (IMU) provided information on the pitch, roll and yaw of the aircraft. The raw data consists of simultaneously recorded laser location and altitude allows reconstruction of the land elevation levels. The data are taken as a 3D point cloud and projected onto a local map datum, sorted and filtered to create a regular grid of elevation values. Greater

information regarding the Lidar system can be found in FASTRAC (2008) and more general discussions in Wehr and Lohr (1999) and Baltsavias (1999).

2.5.2 Airborne Thematic Mapping (ATM)

Airborne multispectral remote sensing was used to assess its suitability at providing information regarding both bedrock and superficial geological features. The study employed data from the NERC archive obtained using a Daedalus Airborne Thematic Mapper 1268 (ATM), taken on 25 June 1996. The survey was originally intended for archaeological investigations along the River Trent. Multispectral imagery works through the examination of discrete spectral bands both within the visible spectrum and beyond into the shortwave and thermal infrared. This allows increased discrimination of earth surface material based on their distinctive spectral reflectance. False-colour images can be produced by combining single spectral bands to each of the red, green and blue colour channels of a computer graphics system. Various false-colour combinations can delineate geological features, lithologies, soil types and palaeochannel architecture.

The Daedalus 1268 ATM records spectral reflectance and infrared radiation in 11 discrete bands of visible blue to thermal infrared wavelength bands (0.42-13μm). Reflectance is recorded on an 8-bit digital scale (image pixel values from 0-255) at a typical resolution of 2m. Data for the study area was downloaded from the NERC archive in HDF format, processed and geocorrected prior to conversion to appropriate formats for analysis. Data was initially converted to Erdas Imagine image format and subsequently into ArcGIS 9.1 grid format for integration into the project GIS. Originally data from the NERC archive were radiometrically corrected but no other post processing was performed. Since no quantitative analysis was to be undertaken it was considered unnecessary to carry out atmospheric correction. Geocorrection was undertaken by pre-processing ATM data using Azimuth Systems Azgcorr 4.8 to combine flight ephemera and radiance data to produce images with real world co-ordinates (OSGB36 co-ordinate system). Where necessary further correction was

undertaken in ArcGIS 9.2 using Ordnance Survey 1: 50000 base map as a source for GCP. False-colour composite (FCC) images were created by displaying combinations of geocorrected image bands within ArcGIS. FCC images using the middle and thermal infrared bands of ATM are especially effective at displaying variations in soil character, such as soil moisture. Images presented from the use of ATM photography use the FCC combination of bands 11-10-5 in red-green-blue.

2.6 Data storage and handling

All datasets used in this study are stored in BGS corporate data stores and are extracted from those stores for spatial analysis and modelling in GSI3D (Williams and Scheib, 2008). Digital Terrain Models are made available as ASCII grids and codified boreholes and augerholes are downloaded from the BGS' corporate Single Onshore Borehole Index (SOBI) and Borehole Geology (BoGe) databases as tabulator separated ASCII files. Geological map data came from DigMapGB, which are held by BGS in proprietary ESRI format. Geophysical results were produced as georeferenced raster images, including horizontal property maps and vertical cross-sectional slices. During the creation of the geological framework model all these datasets were validated, cross-checked and the corporate database was updated iteratively. The resulting geological model was then stored as attributed TINs which define the geological units in their full extent as 3D polyhedra.

3. Results

3.1 Geological survey and creation of initial 3D model

The geology of the area is covered by three main publications, Rathbone (1989), Charsley *et al*., (1990) and Howard *et al*. (In Press). Therefore it is not the intention here to describe the geology in detail. However, some background information and the main features identified from the new geological survey are reported as it forms the basis of the 3D mapping (Figure 1). The bedrock geology of the site is entirely within the Triassic Mercia Mudstone Group. Most of the site is on the Gunthorpe Member of the Sidmouth Mudstone Formation although much is obscured by recent

Quaternary deposits including tills in the SW corner of the model and the terrace deposits (gravel, sands, silts, and clays) of the River Trent. The Edwalton Member caps the escarpment, outcropping in the extreme south-east of the site and is partially obscured by till in the SW corner of the model area. The Cotgrave Sandstone Member forms a significant crest feature and dip slope near the top of the escarpment. It is up to 4 m thick and consists of greenish grey, fine-grained sandstone with subordinate mudstone. Alterations have been made to the originally mapped unit, included widening of this outcrop.

At least 50 m of the Gunthorpe member and 10m of the Edwalton Member are present beneath the site with the upper 25 m of the Gunthorpe Member cropping out in the north-east – south-west trending escarpment that crosses the south-eastern part of the site. Both consist of predominantly red-brown, structureless mudstones. Subordinate lithologies include thin beds of greenish grey, fine-grained, dolomitic sandstone and siltstone beds at intervals, with some beds of laminated mudstone. Three beds of siltstone/sandstone have been mapped across the site on the lower part of the escarpment.

Quaternary deposits included a Middle Pleistocene glacial till that caps the high ground in the south-east of the site. It comprises reddish brown, silty to sandy clay with many pebbles and may be correlated with the Thrussington Till of the Midlands (Rice, 1968). Prior to the terrace deposits, a series of head and colluvium deposits are found covering the Holme Pierrepoint sands and gravels (HPSG). A broad strip of head deposits cross the site, running north-east – south-west at the foot of and parallel to the escarpment. Two boreholes drilled on this deposit reported that the thickness of the head deposits were 1.0-1.25 m. The southern margin of the head is clearly defined by a concave break of slope at the foot of the escarpment; the northern boundary however, is very poorly defined and diffuse, the deposit grading almost imperceptibly into the adjacent HPSG. Head generally forms by solifluction processes although its occurrence at the base of the escarpment will mean some input

from hill wash and soil creep (colluvium). The colluvium deposits were found to be lithologically identical to head, reflecting the Mercia Mudstone and till source rocks. The HPSG form the main terrace of the River Trent at Shelford. It was originally thought that a second terrace existed (Hemington Terrace) from recent work by Carney *et al*. (2001). However, the LIDAR survey (Figure 4) shows that there is only one recognizable terrace of the River Trent, consisting of the HPSG. The terrace consists of brown, fine- to medium-grained non-micaceous sand that is clayey in the upper part and becomes generally more clayey and locally a silt closer to the River Trent. Boreholes demonstrated that the thickness of the deposit was up to 5.4 m thick and rests with a sharp angular base on the Mercia Mudstone. The upper part of the terrace is variably sandy clay or sand, to depths of 1.8-2.35 m. The lower part of the terrace is poorly sorted gravel, locally with very sandy layers.

Recent alluvial sand deposits crop out at the extreme northern end of the site as a narrow strip less than 100 m wide (Figure 1). This deposit is a brown, micaceous sand that becomes clayey at around 0.8 m in the banks of the Trent. Older alluvial deposits (Holocene) are found within the HPSG (Figure 1) in the nature of alluvial clay, silt and sand. An outcrop of alluvium forms a narrow c. 100 m wide strip crossing the HPSG and trending north-east – south-west. This deposit forms a slight topographic low on the river terrace and the deposit is up to 1 m thick. A second area of alluvial clay, silt and sand occurs in a narrow tributary valley trending south-west – north-east and running immediately south-east of Shelford village (Figure 1). It is clearly defined by a slight topographic low on the surface of the river terrace. It consists of grey silty to sandy clay and sandy clayey silt and is up to 1 m thick. North eastwards, the alluvium dies out as the stream cuts down into the HPSG. The third area of alluvial clay, silt and sand occurs along the north-eastern margin of the site area. It is marked by a very slight depression and is red brown sandy clay ~ 0.7 m deep. These tracts of alluvium crossing the river terraces are thought to mark former channels of the River Trent.

A first version of the model was constructed in GSI3D utilising a NEXTmap DTM (5m cell size), re-mapped geological linework and the mapped polygons at a scale of 1:10,000 and borehole log data from 35 locations across the study area. The locations of the boreholes used are shown on Figure 2D where the geological sections intersect.

3.2 The enhanced 3D model

The initial model served as a preliminary geological framework of the subsurface of the study area. The model was further refined and improved by incorporating results of the shallow geophysical investigations. The following sub-sections provide examples of areas where the model and understanding of the subsurface was improved by the incorporation and/or collection of geophysical and remote sensing data.

3.2.1 Example 1: The Buried Cliff

Traditional geological survey and borehole logs established that a transition existed between the Mercia Mudstone escarpment and the sand and gravel terrace deposits. However, as a result of the wide spacing between boreholes, the gravels were originally interpreted as gradually thinning out towards the slope of the Gunthorpe Member as no further information was available. The ARP survey data acquired across the southern extent of the site identified a sharp linear resistivity contrast along the base of slope (Figure 5), where the more conductive soils-sediments of the Gunthorpe Formation mudstones on the slope are replaced by the more resistive soils-sediments of the river terrace. This feature was located near the base of the slope and was identified by the ARP survey to extend over a significant distance across the surveyed area (Figure 5). Whilst the ARP data enabled this feature to be mapped laterally along the slope in an E-W direction, the use of ERT enabled the vertical extent of the feature to be defined with greater certainty (Figure 5 and 6). The main ERT traverse (Figure 6) across the slope identifies a buried cliff in the Gunthorpe Member, ~3 m deep, in-filled with deposits (HPSG) of a higher resistivity ($60 \leq \rho \leq 260$ Ωm). Borehole logs demonstrated an almost pure sand deposit close to the cliff with a maximum resistivity >100 Ωm.

This is then surrounded by material with a slightly lower resistivity (~100 Ωm), eventually grading into a more conductive material (40-60 Ωm) which appears to be more typical of the resistivity of the HPSG, thus being a mixture of sand and gravel.

In the initial model, the HPSG were mapped assuming a gradual thinning and without the sharp boundary defined by the ARP and ERT surveys. The enhanced model takes into account the geophysical data acquired at the site, allowing for modification of the geological cross-sections in the fence-diagram. Figure 5 illustrates how the geophysical data have been used to aid the 3D mapping of the feature through the construction of geo-referenced parallel and intersecting cross sections. The ATM image (Fig 7) also reveals the buried cliff-line.

3.2.2 Example 2: Siltstone Bed mapping

Siltstone beds are an important geological feature in both the Gunthorpe and Edwalton members of the Mercia Mudstone Group. Their accurate mapping is important for construction purposes and their presence close to the surface can potentially affect the soils moisture regime. Within conventional geological surveys their presence is mapped as topographic features where they outcrop. In the present study, the ARP, ERT and ATM surveys were all found to produce more detailed information relating to their presence. In the 2D ERT models (Figure 6), the siltstone beds appear as marked features with higher resistivities compared to the Gunthorpe Member in which they reside. The elevated resistivities may be a function of the harder texture, lower porosity and hence lower pore water content of the siltstone. The ARP survey also identified the siltstone beds as thin bands of resistive material following the topography of the escarpment (Figure 8) and allows for improved mapping. Remote sensing ATM images reveal the study site and surrounding area in a wider context as part of the Trent valley landscape. Figure 7 has been geo-referenced and the annotations show the extent of the buried cliff along the valley and where it eventually ends close to the village of East Bridgford. The end of the cliff appears to coincide with the presence of the much

harder siltstone beds that are found within the Gunthorpe Member. Thus it can be surmised that the buried cliff feature represents the maximum south easterly incision of the River Trent within the study area with the siltstone beds acting as the controlling factor in determining the extent of the floodplain.

3.2.3 Example 3: Variability of the HPSG deposits

Another area where the application of geophysical survey techniques benefitted the mapping and interpretation of geological units within the 3D model was in assessing the spatial variability of the HPSG units that are usually mapped as one geological unit. The HPSG deposits typically consist of poorly-sorted, clast-supported gravel, 6 to 9 m thick, with a medium- to coarse-grained sand matrix, interstratified with lenses of medium- to coarse-grained sand and pebbly sand. Pebbles are generally less than 50 mm across, but there are larger ones that range up to 0.1 m.

The apparent resistivity maps acquired using the ARP technique display a high degree of lateral variation in the resistivity values of the near-surface across the site (Figure 9). The dominant controls over resistivities on the flood plain are thought to be grain size and clay/silt content, so that the ARP maps can be used to infer the nature of the shallow deposits. The heterogeneity within the river terrace deposits displayed by these maps has been attributed to the distribution of gravel-rich (i.e. resistive) sand and gravel deposits (red), with sand-rich (i.e. relatively more conductive) sand and gravel deposits being represented on the maps by yellow through green. Relatively high resistivity values (red) were found to correspond to slightly raised areas of coarse sandy gravel. Raised gravel bars within the river terrace deposits were originally identified from surface topography and are an expected feature in braided river systems. In addition, the use of ATM photography and images using the FCC combination of bands 11-10-5 in red-green-blue was especially good at revealing lithological variations of clays (dark) in topographic depressions and coarse sand and gravels (light) on gentle topographic ridges in the River Trent alluvial flood-plain.

Figure 10 in particular highlights the shape and likely textural variations in the sand and gravel bars in the meander to the west of the study site.

One feature in particular that was identified within the HPSG by the ARP survey is marked on Figure 9 as the Moors Plantation. This was identified as a very coarse cobbly gravel as indicated by the relatively high resistivity values from the ARP survey. This probably represents an elongated palaeo-island that ran parallel to the incised buried channel and palaeo-cliff line, marking the southern boundary of the Devensian Trent valley. Roberts *et al.* (1997) describe GPR profiles across a modern gravel bar of the River Rhone, in which accreted islands up to 1 km long are separated by abandoned channels filled with sand or silty sand during high river discharges. However, the identified palaeo-island in this study is much smaller and is only 600 by 200 m.

GPR surveys were also undertaken in the HPSG (Figure 11). The GPR 100 MHz antenna data shows little sedimentological detail in the top ~1.5 m due to a combination of a clayey sub-soil causing signal attenuation and the masking effect of the first strong (high amplitude) reflector caused by the water table. However, good reflective detail is generally observed in the saturated zone. Again, because of signal attenuation a relatively weak radar reflection at the base of the radargrams (~ 5-6 m) marks the contact with the weathered mudstone bedrock (Gunn *et al*., 2005). It is possible to corroborate the thickness of the sand and gravel deposit observed in the ERT sections (e.g. the flat- lying bedrock reflector seen in Figure 14), but impossible where reflections are absent due to a relatively thick overlying clay or uniform sand. The results from the higher frequency 250 MHz Noggin were generally poor due to a lack of reflectivity and penetration (~ 1m) as the sediments above the water table were often clayey and relatively conductive. Additional information that could have been included from the GPR data such as the position of the water table, as well as plotting individual geological beds and layers using individually picked horizons were not

included. This was because only a limited number of GPR transects were undertaken. However, if such information was required by the model the use of GPR and ERT data could be incorporated.

3.3 General Discussion

The results have demonstrated how the integrated geophysical and remote sensing surveys have increased the resolution of the geological mapping and development of the 3D geological model. However, the integrated surveys have also produced considerable information to enhance our knowledge of the complexity and history of the sedimentary environments of the terrace deposits at Shelford. The current course of the River Trent was thought to have been initiated during the Late Anglian deglaciation, where a structural weakness was exploited between the Pennine and Eastern ice sheets (Howard et al. *In press*). Thus, a series of terrace deposits exists across the Trent Valley, dating from the Anglian onwards (Howard et al. *In press*). Knowledge of the depositional environments of the Trent valley has largely been obtained from numerous borehole surveys of the sand and gravel resources and inspection of geological exposures at their extraction sites. Previously, only one GPR survey of the Trent Valley has been published on the fluvial deposit architecture in terraces of the Upper Trent (Davies and Sambrook Smith, 2006).

The HPSG is the youngest of the Quaternary terraces that are found within the Trent Valley and has been dated at ~24000 yrs BP or Marine Isotope Stage (MIS) 2 (Howard *et al*., *In press*). Much of the material that forms this terrace originated from the reworking of earlier terraces and from the Sherwood Sandstone outcrop to the north. The latter was moved by periglacial mass wasting processes through the Pleistocene. The material reworked from the older terraces was largely sourced from glacial deposits. Like the deposits studied by Davies and Sambrook Smith (2006), they were probably formed by aggradation in a glacial meltwater-charged, braided river system. Continuous permafrost with highly seasonal water discharges combined with the absence of vegetation and permafrost induced landscape instability would produce a high sediment supply.

This resulted in aggradation across a very unstable floodplain (Mol *et al*., 2000) and is similar to the depositional environment suggested by Davies and Sambrook Smith (2006) in the Upper Trent. Further evidence of this depositional regime includes truncated ice wedge casts found 10 km down stream at Hoveringham corresponding to the Late Devensian Stadial (Howard, 1992) and deposits recently uncovered at Holme Pierrepont, 10 km upstream, that feature tabular to very broadly lenticular bodies of sand and gravel that are laterally continuous over scales of several to tens of metres. In these deposits foreset beds are typically gently inclined, in keeping with deposition as low-profile bars that formed within a braided river system subject to seasonally high discharges. Abandoned watercourses were filled with organic-rich and peaty material. One such lens has been uncovered during recent excavations at Holme Pierrepont.

The identification of several important terrace features through our integrated geophysical survey has added to the interpretation of the sedimentary history of the Trent Valley. In our study 'the buried cliff' line identified through both the ARP survey and the ATM photos represents the southern most edge of the braided river system in section of the Trent Valley. There is a strong possibility that the identified siltsone beds provide an erosion resistant river bank that constrained the southward erosion of the Gunthorpe Member to the east of the site at East Bridgford. At this point the HPSG terraces on the southern side of the river have disappeared (Figure 7). Adjacent to the buried cliff, a sand filled channel was located through the ERT profile (Figure 6) and was confirmed by a number of boreholes. This predominantly sand filled channel, overlain by head deposits is unusual as the HPSG is typically gravel-rich with clasts. The sand filled channel was ~2.5 m deep and infilled with a sequence of predominantly fine to medium grained sand showing two upward fining cycles defined by gravely bases. The sand channel is assumed to have been cut and abandoned during formation of the terrace and later infilled. The dominant sand lithology might suggest a late stage fill when the flow regime was slower and the bed load much finer, the repeated fining upward cycles, from gravel to sand suggesting a more meandering fluvial environment.

The lateral complexity of the depositional environments of the HPSG deposits was demonstrated by the ARP surveys. Several areas of high resistivity associated with increases in gravel content were identified across the surveyed area (Figure 9). Combined GPR and ERT transects were taken to assess and investigate depth and depositional features of the HPSG (Figure 3). In near-surface investigations GPR can provide a high degree of vertical and horizontal resolution, ideally complementing the ERT technique (Slater and Reeve, 2002), as they are each controlled by contrasts in different electrical parameters (permittivity and, resistivity respectively). Thus, GPR data did add detailed sedimentary information to the ERT sections and hence, has improved the overall interpretation of the Trent Quaternary Fluvial system.

In Figures 12, 13 and 14 the detailed GPR radargrams are shown side by side with corresponding ERT sections. The joint interpretations give an indication of the size and position of Pleistocene and Holocene palaeochannels. Figures 12 and 13 comprise a continuous south-north down slope section of ~920m in length (Lines 2 and 3, Figure 3). The ERT models indicate a 5-6 m thick quaternary sand and gravel deposit overlying a relatively planar bedrock surface of Mercia Mudstone (indicated by blue colour of ~ < 35 Ωm on ERT sections). The southern boundary (Figure 12) of the sand and gravel deposit is marked by a sinuous buried channel along the edge of the buried cliff (Figure 6), which was proved by a series of boreholes. The dipping reflectors observed on the GPR radargram at 96 m can be interpreted as the northern edge of this channel (indicating an approximate width of 150m to 'the buried cliff'). This feature is only subtly indicated on the ERT section. The lack of GPR reflections within this part of the channel proves the infilling sand deposits are relative uniform and homogenous. A change in radar facies is noted from ~225 m to the end of the section (Figure 12) where fine scale diffractions denote a presumed relatively thin deposit of pebbles (possibly imbricated) overlying a silty sand at a depth of ~2 m. The alluvial channel reported in Figure 13 is considered to be a Holocene deposit. The deposition of alluvium requires much slower water than is required to produce the Pleistocene palaeochannels and the channel probably

represents a side stream of the River Trent. The resistivity of the alluvial deposit is ~70 Ωm and is found between 210 – 305 m on Figure 13. The corresponding GPR section indicates continuous near-horizontal reflectors, typical of a low energy slack water silty clay deposit. The apparent erosional depression observed in the underlying Mercia Mudstone, indicates that this may have been a much wider channel (165 – 315 m) in the past. The gravel bars mapped either side of this feature are characterized by their relatively high resistivities (> 150 ohm m). Dipping reflectors on the flanks of these bars suggest growth by lateral accretion. Figure 13 also shows scour filled channels at centres of ~350 and 490 m.

Figure 14 shows an adjacent section 500m to the west (Line 4, Figure 3). Interpretation of the radargram indicates palaeochannels (~70 - 100 m wide) either side of the 120 m wide gravel bar with reduced resistivities noted in the corresponding ERT section. Thus the GPR and ERT have identified the position and width of a series of Quaternary and Holocene palaeochannels and deposits across the study site that enhances the geological mapping.

4. Conclusions

This study has used a combination of geological survey, borehole logs, geophysical survey and remote sensing to produce a high resolution 3D geological model and interpretation of fluvial processes at Shelford. The combination of the different geophysical surveys has enabled several geological and geomorphological features to be identified that would have remained undetected or poorly mapped using standard geological survey and borehole analysis to create the 3D model. The study has shown that in order to gain an improved understanding of the shallow subsurface and for 3D mapping of complicated systems such as floodplains and terraces it is vital to use and integrate all available geological, geophysical and remote sensing tools and methodologies. In particular, it was found that the ARP survey was essential in identifying unobserved features, because the technique could survey several hectares a day. What has hampered an integrated whole system

approach to studies of this kind in the past was that the data from different surveys were presented in different data formats and associated software tools. It was therefore not possible to synthesise all available information in one common virtual environment, which enabled all scientists involved to view the data in an integrated manner. However, GSI3D is an intuitive tool for geological modelling particularly well suited for near surface geoscientific investigations. It allows a wide range of geoscientists who are not necessarily IT experts to work together and visualise and analyse their respective data and measurements in a 3D context. Technically Gocad and other oil industry standard software could be used for this task, but they are inherently complex to use and not widely available to BGS scientists. GSI3D basically fulfils the function of a GIS in integrating and visualising data, not in 2D but in 3D. Recently, the GSI3D methodology and software has become available to earth scientists worldwide through the GSI3D research consortium (www.GSI3d.org.uk)..

5. Acknowledgements

The authors would like to thank all of the members of the Sustainable Soils 3D Modelling Team who contributed to the gathering of the data at Shelford. In particular, we would like to thank Miroslav Vrzba who undertook much of the geophysical processing. We would also like to thank the Geomatics Group 2009 for allowing us to use the Lidar image of the Shelford area and the farmers who allowed access to their land. The paper is published with the permission of the Director of the British Geological Survey.

References

Anderson, S.P., von Blanckenburg, F. and White, A.F. 2007. Physical and chemical controls on the Critical Zone. *Elements*, **3**, 315-319.

Annan, A.P. and Davis, J.L., 1976. Impulse radar sounding in permafrost. *Radio Sci.*, **11**, 383-394.

Annan, A.P., 1993. Practical processing of GPR data. Sensors and Software, Inc.

Baltsavias, E.P. 1999. Airborne laser scanning: basic relations and formulas. *ISPRS Journal of Photogrammetry and Remote Sensing* 54, 199-214.

Brantley, S.L., Goldhaber, M.B. and Ragnarsdottir, K.V. 2007. Crossing disciplines and scales to understand the critical zone. *Elements*, **3**, 307-314.

Carney, J N, Ambrose, K, and Brandon, A. 2001. Geology of the country between Loughborough, Burton and Derby. *Sheet Description of the British Geological Survey,* 1:50 000 Series Sheet 141 Loughborough (England and Wales).

Chambers, J.E., Wilkinson, P.B., Weller, A.L., Aumonier, J., Ogilvy, R.D., Williams, J.D.O., Meldrum, P.I. and Kuras, O. 2008. Determining Reserves of aggregates by non-invasive electrical tomography (DRAGNET). MIST project MA/6/1/008. *British Geological Survey Commissioned Report CR/08/040*. 64pp.

Charsley, T.J., Rathbone, P.A. and Lowe, D.J., 1990. Nottingham: a geological background for planning and development. *BGS Technical Report WA/90/1*.

Dabas, M., 2009. Theory and practice of the new fast electrical imaging system ARP. In: Seeing the Unseen. Geophysics and Landscape Archaeology; Campana S. and Piro S. (eds). CRC Press, London, 105-126.

Dabas, M. and Favard, A. 2006.Rapid electrical soil mapping at Shelford, Nottinghamshire, UK. Phase 1 pilot survey – October 2006. *Geocarta commissioned report for British Geological Survey*. 25pp.

Dabas, M. and Favard, A. 2007. Rapid electrical soil mapping at Shelford, Nottinghamshire, and five further sites across the UK. Phase 2 ARP survey – February 2007. *Geocarta commissioned report for British Geological Survey*. 26pp.

Dabas, M. and Tabbagh, A., 2003. A comparison of EMI and DC methods used in soil mapping - theoretical considerations for precision agriculture. Precision agriculture: Papers from the 4th European Conference on Precision Agriculture, Berlin, Germany, 15-19 June 2003.

Dahlin, T., 1996. 2D resistivity surveying for environment al and engineering applications. First Break, 14 (7), 275-283.

Davis, J.L. and Annan, A.P., 1989. Ground-penetrating radar for high-resolution mapping of soil and rock stratigraphy. *Geophysical Prospecting*. **37**, 531-551.

Davies, N.S. and Sambrook Smith, G.H. 2006. Signatures of Quaternary fluvial response, Upper River Trent, Staffordshire, U.K.: A synthesis of outcrop, documentary, and GPR data. Geomorph. N.F., 50, 347-374.

FASTRAC. 2008. A whole-site first–assessment toolkit for combined mineral resource and archeological assessment in sand and gravel deposits. *The FASTRAC Project – Final Report*. Hill, I. (ed). ALSF Research Project PN 5366.

Fisher, T.G., Jol, H.M., and Smith, D.G., 1995. Ground penetrating radar used to assess aggregate in catastrophic flood deposits, N.E. Alberta, Canada: Canadian Geotechnical Journal, v. 32, p. 817–879.

Gourry, J.C., Vermeersch, F., Garcin, M. and Giot, D. 2003. Contribution of geophysics to the study of alluvial deposits: a case study in the Val d'Avaray area of the river Loire, France. Journal of Applied Geophysics, 54, 35-49.

Green, P.J. and Sibson, R. 1978. Computing Dirichlet tessellations in the plane. Computer Journal **21** (2), 168–173.

Gunn, D. A., Nelder, L. M., Pearson, S., Thompson, G., Carney, J. N. and Wallis, H. 2005. Investigating shear wave methods to characterize sand and gravel thicknesses at Holme Pierrepont, Nottingham. British Geological Survey. Internal Report IR/03/116.

Howard, A. J. 1992. The Quaternary geology and geomorphology of the area between Newark and Lincoln. Unpublished PhD thesis, University of Derby.

Howard, A S, Warrington, G, Ambrose, K, Carney, J N, Young, S R, and Pharaoh, T C. *In press.* Geology of the country around Nottingham. *Memoir of the British Geological Survey*, Sheet 126 (England and Wales).

Hugenholtz, C.H., Paulen, R.C. and Wolfe, S.A. 2007. Ground penetrating-radar investigation of relict channel bars of the Meander River spillway, northern Alberta. Geological Survey of Canada, Current Research, 2007-A1, 10pp.

Huggenberger, P. 1993. Radar facies: recognition of facies patterns and heterogeneities within Pleistocene Rhine gravels, NE Switzerland. From Best, J. L. and Bristow, C. S. (eds), 1993, Braided Rivers, Geological Society Special Publications No. 75, pp. 163-176.

Hughes AG, Graham MT, Jackson CR, Mansour MM and Vounaki T, 2008. ZOOM into GSI3D: Using 3D geological models to better parameterise groundwater models. In Mathers, S.J. (editor), Extended Abstracts of the 2nd International GSI3D conference, 2-3rd September 2008. British Geological Survey Open File Report (OR/08/054), 30pp. http://nora.nerc.ac.uk/4477.

Jol, H.M., Parry, D., and Smith, D.G. 1998. Ground penetrating radar - Applications in sand and gravel exploration, in Bobrowsky, P.T., ed., Aggregate resources - A global perspective: Rotterdam, Netherlands, A.A. Balkema, Inc., p. 295–306.

Jol, H. M. and Bristow, C. 2003. GPR in Sediments: advice on data collection and basic processing and interpretation, a good practice guide. Pp. 9-29 in Bristow, C. J. and Jol, H. M. (Eds) Ground Penetrating Radar in Sediments, The Geological Society, London.

Kessler, H. and Mathers, S.J. 2004. Maps to Models. *Geoscientist*, **14/10**, 4-6.

Kessler, H., Mathers, S.J. and Sobisch, H.-G. 2009. The capture and dissemination of integrated 3D geospatial knowledge at the British Geological Survey using GSI3D software and methodology. Computers and Geosciences, 35, 1311-1321.

Kuras, O., Meldrum, P.I., Beamish, D., Ogilvy, R.D. and Lala, D., 2007. Capacitive resistivity imaging with towed arrays. Journal of Environmental and Engineering Geophysics, 12(3): 267-279.

Lelliott, M.R., Bridge, D.M., Kessler, H., Price, S.J. and Seymour, K.J. 2006. The application of 3D geological modelling to aquifer recharge assessments in an urban environment. Quarterly Journal of Engineering Geology and Hydrogeology, 39, 293-302.

Loke, M., 2007. RESDINV version 3.56 Software Manual, Geotomo Software. http://www.geoelectrical.com/ Accessed on 03/03/2009

Lunt, I.A. and Bridge, J.S. 2004. Evolution and deposits of a gravelly braid bar, Sagavanirktok River, Alaska. Sedimentology, 51, 415-432.

Lunt, I.A., Bridge, J.S. and Tye, R.S. 2004. A quantitative, three-dimensional depositional model of gravelly braided rivers. Sedimentology, 51, 377-414.

McCuaig, S.J., and Ricketts, M.J., 2004. Ground-penetrating radar—A tool for delineating aggregate-resource deposits: Newfoundland and Labrador Department of Mines and Energy, St. John's, Newfoundland, Geological Survey Report 04–1, p. 107–115.

Macmillan, A.A., Heathcote, A.J., Klink, B.A., Shepley, M.G. Jackson, C.P. and Deglen, P.J. 2000. Hydrogeological characterisation of the onshore quaternary sediments at Sellafield, U.K. using the concept of domains. *Quarterly Journal of Engineering Geology and Hydrogeology*, **33**, 301- 323.

Merritt J, Monaghan, A., Entwistle D, Hughes AG, Campbell D and Browne M, 2007, 3D attributed models for addressing environmental and engineering geoscience problems in areas of urban regeneration – a case study in Glasgow, UK. First Break, 25, 8 (August), 79-84.

Mol, J., Vandenberghe, J. and Kasse, C. 2000. River response to variations of periglacial climate in mid-latitude Europe.

Newell, A.J. 2007. Morphology and Quaternary geology of the Thames floodplain around Oxford. British Geological Survey Open Report, OR/08/030. 30 pp.

Neal, A. 2004. Ground-penetrating radar and its use in sedimentology: principles, problems and progress; Earth Sci. Rev. 66 261–330.

Panissod, C., Dabas, M., Hesse, A., Jolivet, A., Tabbagh, J. and Tabbagh, A., 1998. Recent developments in shallow-depth electrical and electrostatic prospecting using mobile arrays. Geophysics, 63(5): 1542-1550.

Pipan, M., Baradello, L., Forte, E., Prizzon, A., Finetti, I., 1999. 2-D and 3-D processing and interpretation of multi-fold ground penetrating radar data: a case history from an archaeological site. J. Appl. Geophys. 41, 271– 292.

Rathbone, P A. 1989. Geology of the East Bridgford district. *British Geological Survey Technical Report,* WA/89/16.

Rice, R J. 1968. The Quaternary Era. 332–355 in *The Geology of the East Midlands*. Sylvester-Bradley. P C, and Ford, T D (eds), Leicester University Press.)

Roberts, M.C., Bravard, J. and Jol, H.M. 1997. Radar signatures and structure of an avulsed channel: Rhone River, Aoste, France. J. Quatern. Sci., 12, 35–42.

Samouelian, A., Cousin, I., Tabbagh, A., Bruand, A. and Richard, G., 2005. Electrical resistivity survey in soil science: a review. Soil and Tillage Research, 83(2): 173-193.

Scheib A. J., Ambrose K., Boon D. P., Kessler H., Kuras O., Lelliott M., Nice S. E., Palmer R. C., Raines M. G., Smith B. 2007. 3D Digital Soil-Geology Models of the Near Surface Environment; Abstract for Pedometrics Biannual Conference of Commission 1.5 Pedometrics, International Union of Soil Sciences, Germany. p85. https://archive.ugent.be/retrieve/4564/Book+of+Abstracts.pdf

Slater, L.D. and Reeve, A., 2002: Investigating peatland stratigraphy and hydrogeology using integrated electrical geophysics. Geophysics, 67, 365-378.

Smith, B.; Kessler, H.; Scheib, A.J.; Brown,S.E.; Palmer,R.C.; Kuras,O.; Scheib,C., Jordan, C.J. 2008. Chapter 16: 3D Modelling of Geology and Soils – A case study from the UK. Digital Soil Mapping with Limited Data. A. E. Hartemink, A. B. McBratney and M. L. Mendonca-Santos. Berlin, Springer, 183-191p, ISBN 978-1-4020-8591-8.

Van Overmeeren, R.A. 1998. Radar facies of unconsolidated sediments in Netherlands: A radar stratigraphy interpretation method for hydrogeology. Journal of Applied Physics, 40(1-3), 1-18.

Wehr, A. and Lohr, U. 1999. Airborne laser scanning – an introduction and overview. *ISPRS Journal of Photogrammetry and Remote Sensing* 54, 68-82.

Williams J.D.O. and Scheib A.J., 2008. Application of near-surface geophysical data in GSI3D – case studies from Shelford and Talla Linnfoots. British Geological Survey. Open Report Series. OR/08/068. Available on-line: http://nora.nerc.ac.uk/5347/1/OR_08_068.pdf

Young, R.A., Deng, Z., Sun, J., 1995. Interactive processing of GPR data. The Leading Edge 14, 275–280.

List of Captions titles:

Figure 1: Shelford study area and geology. Scale is km of the British National Grid based upon OS topography © Crown Copyright. All rights reserved. BGS 1000017897/2009.

Figure 2: Simplified workflow for the construction of a 3D model using GSI3D. The methodology utilizes A) geological outcrop data (linework and polygons), B) classified borehole data and C) a digital terrain model (DTM). The user draws intersecting cross-sections between boreholes correlating the lateral and vertical extent of the geological units, resulting in D) a fence diagram. Triangulation of latter with the boundaries of all geological units computes a 3D model (E) made up of individual geological volumes.

Figure 3: Map showing locations of geophysical surveys including Automated Resistivity Profiling (ARP), Ground Penetrating Radar (GPR) and Electrical Resistivity Tomography (ERT). The location of the Common Mid Point (CMP) velocity analysis for the GPR survey is also shown. The numbers correspond to ERT and GPR survey lines shown in Figures 6, 11, 12, 13 and 14. Scale is km of the British National Grid based upon OS topography © Crown Copyright. All rights reserved. BGS 1000017897/2009.

Figure 4: LIDAR image of the Shelford study site. The image shows the extent of the step down from the Holme Pierrepont terrace (2) to the modern alluvial floodplain (1). LIDAR data copyright Geomatics Group 2009 and scale is km of the British National Grid based upon OS topography © Crown Copyright. All rights reserved. BGS 1000017897/2009.

Figure 5: Image from GSI3D 3D window showing vertical drop of 3 m shown by ERT pseudo-sections and ARP Channel 1 property map (scale 13-300 Ωm) along with digitised geological cross-sections. Figure 5a and 5b show the same area. Figure 5a shows how the geology would appear if 3D geological model was based solely on geological survey. Figure 5b shows how the 3D geological model is constructed utilising the results of geophysical surveys. Hence the cross-sections in the model were modified in order to display an abrupt vertical drop of 3 m rather than a gradual thinning out of the HPSG towards the slope. The shaded grey area on the inset map shows the area the figure covers.

Figure 6: 2D ERT model along the slope of the Shelford escarpment. Its location is shown on Figure 3 as line (1).

Figure 7: ATM images of bands 11-10-5 in red-green-blue for (a) the Shelford-Gunthorpe-East Bridgford area. The buried cliff-line (arrowed) and the overlying Gunthorpe Formation, is well imaged. The shaded grey area on the inset map shows the area the photo covers.

Figure 8: ARP Maps (Channel 1; 0-0.5 m depth) plotted across a range of 13-300 Ωm and superimposed over the revised geological survey line work. The geophysical image shows distinct linear variations in near-surface deposits that have been interpreted as siltstone beds of the Gunthorpe Member. The ARP survey demonstrates that the mapping position can be improved as compared to the routine geological survey positioning. The shaded grey area on the inset map shows the area the figure covers.

Figure 9: Screenshot of GSI3D 2D window (left) showing horizontal ARP resistivity maps presenting a highly variable distribution of sands and gravels within the HPSG deposits. Areas with green mesh lines represent correlated envelopes / TINs outlining these gravel-rich areas. Black lines are cross sections and thicker, red lines indicate location of key geophysical sections. The 3D model (right) shows the volumes of these gravel-rich HPSG deposits as modelled. The shaded grey area on the inset map shows the area the figure covers.

Fig 10: ATM images of bands 11-10-5 in red-green-blue for the west of the study site showing meander scroll deposits NW of Shelford consisting of clay (dark) in depressions, and coarse sand and gravels (light) forming ridges. The shaded grey area on the inset map shows the area the photo covers.

Figure 11: GPR section across a gravel bar (Southern half of Line 3 in Figure 3).

Figure 12: Images of a) GPR and b) ERT section along main transect (Line 2 in Figure 3).

Figure 13: Images of a) GPR and b) ERT sections along main transect (Line 3 in Figure 3).

Figure 14: Images of a) GPR and b) ERT sections along Line (4) of Figure 3.

Figure 1:

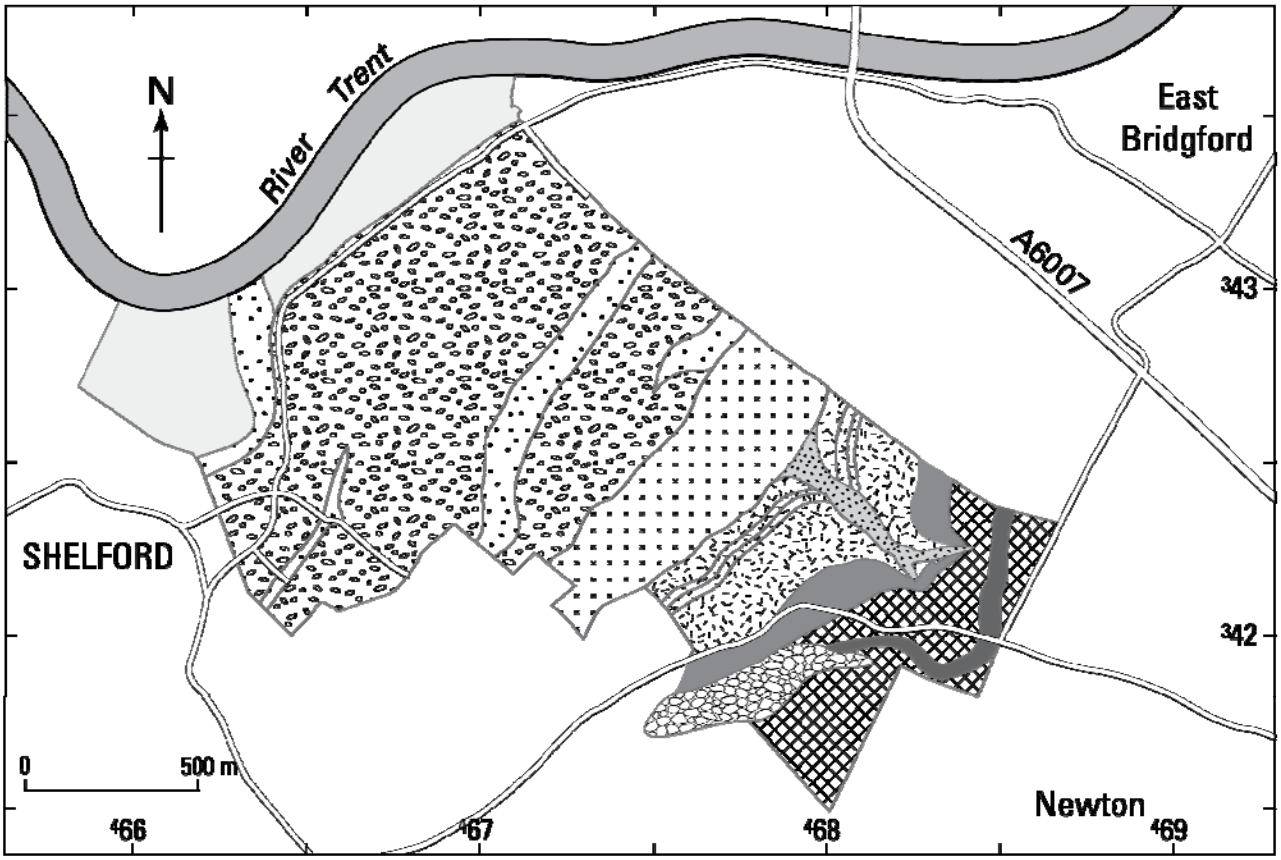

Alluvial sand

Alluvial clay

Holme Pierrepoint Sand and gravel

Head over sand

Colluvium

Gunthorpe Formation with Siltsone Skerries

Cotgrave Sandstone

Edwalton Formation Mudstone

Edwalton Formation Siltstone

Till

Figure 2:

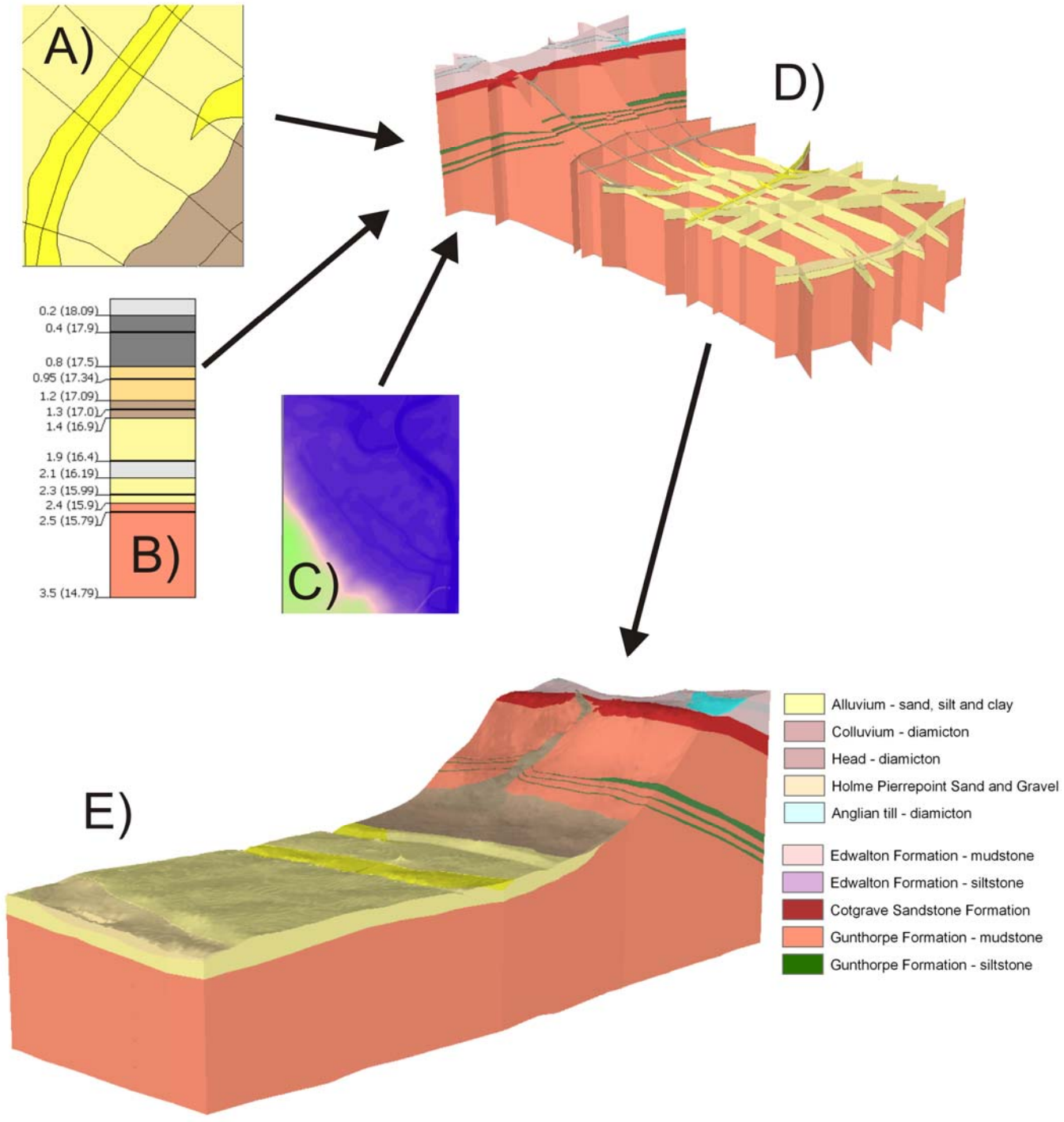
A)
B)
C)
D)
E)
0.2 (18.09)
0.4 (17.9)
0.8 (17.5)
0.95 (17.34)
1.2 (17.09)
1.3 (17.0)
1.4 (16.9)
1.9 (16.4)
2.1 (16.19)
2.3 (15.99)
2.4 (15.9)
2.5 (15.79)
3.5 (14.79)
Alluvium - sand, silt and clay
Colluvium - diamicton
Head - diamicton
Holme Pierrepoint Sand and Gravel
Anglian till - diamicton
Edwalton Formation - mudstone
Edwalton Formation - siltstone
Cotgrave Sandstone Formation
Gunthorpe Formation - mudstone
Gunthorpe Formation - siltstone

Figure 3:

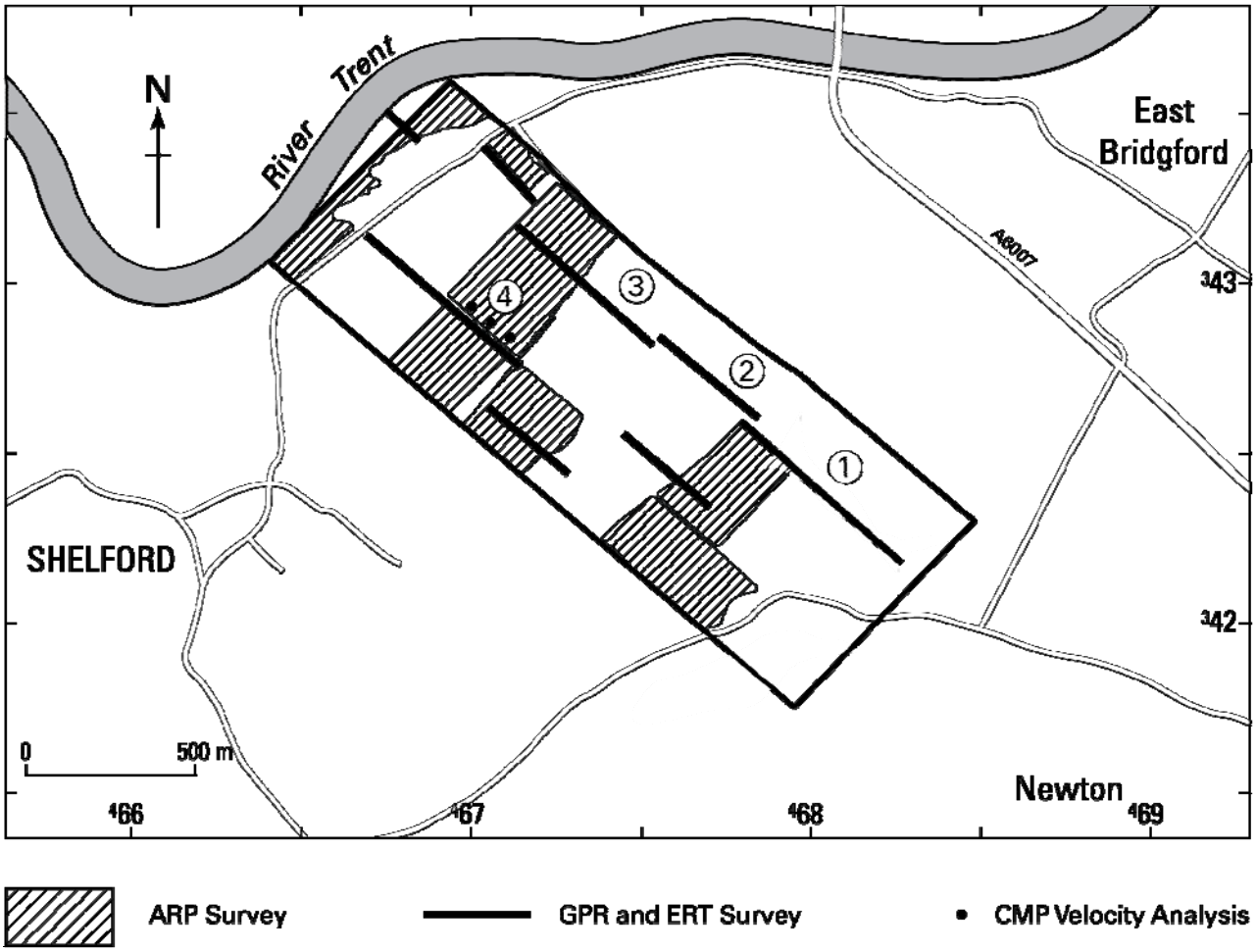
N
River Trent
East
Bridgford
A6097
343
342
SHELFORD
Newton
0
500 m
466
467
468
469
1
2
3
4
ARP Survey
GPR and ERT Survey
CMP Velocity Analysis

Figure 4:

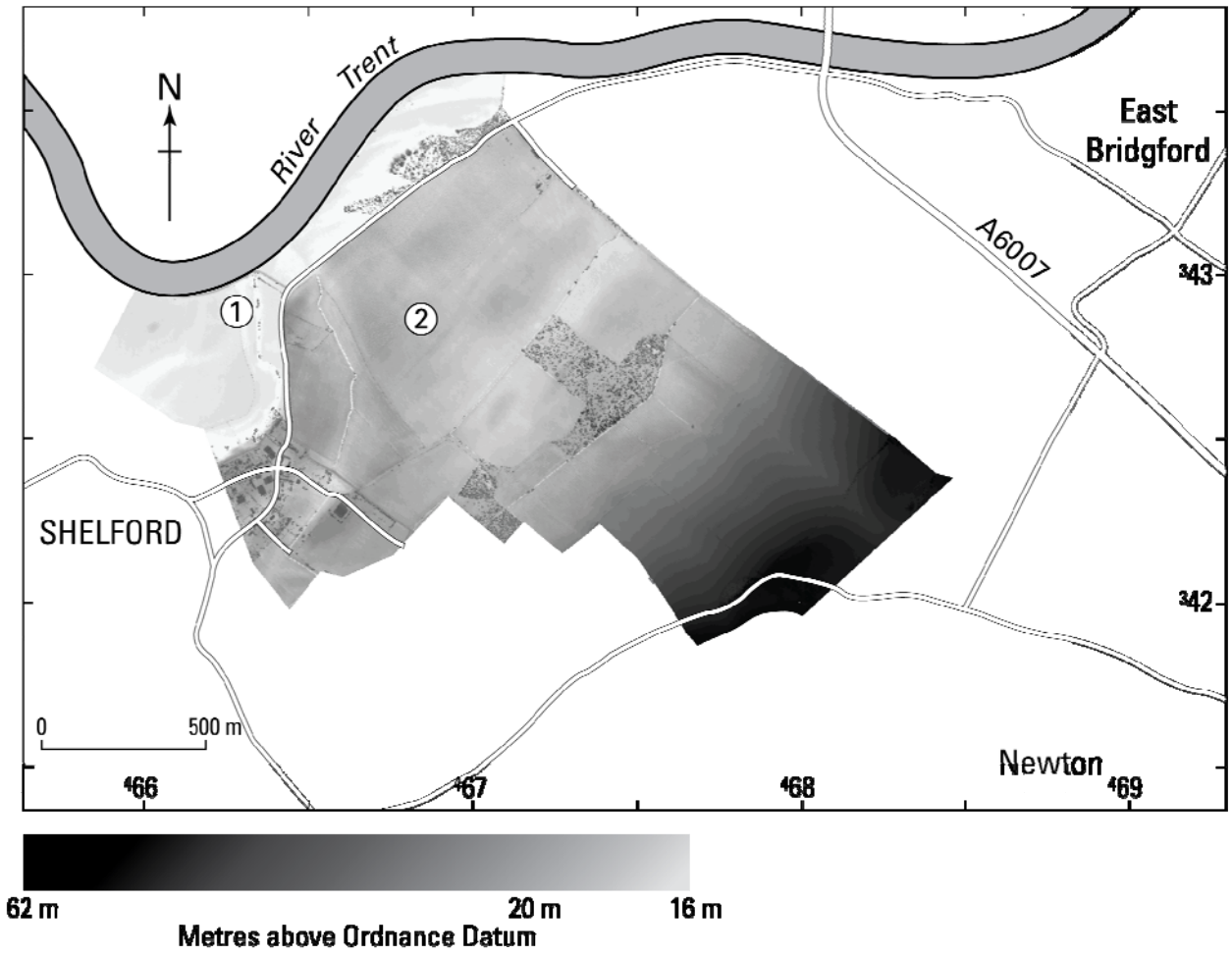
N
River Trent
East Bridgford
A6007
343
1
2
SHELFORD
342
0
500 m
Newton
466
467
468
469
62 m
20 m
16 m
Metres above Ordnance Datum

Figure 5:

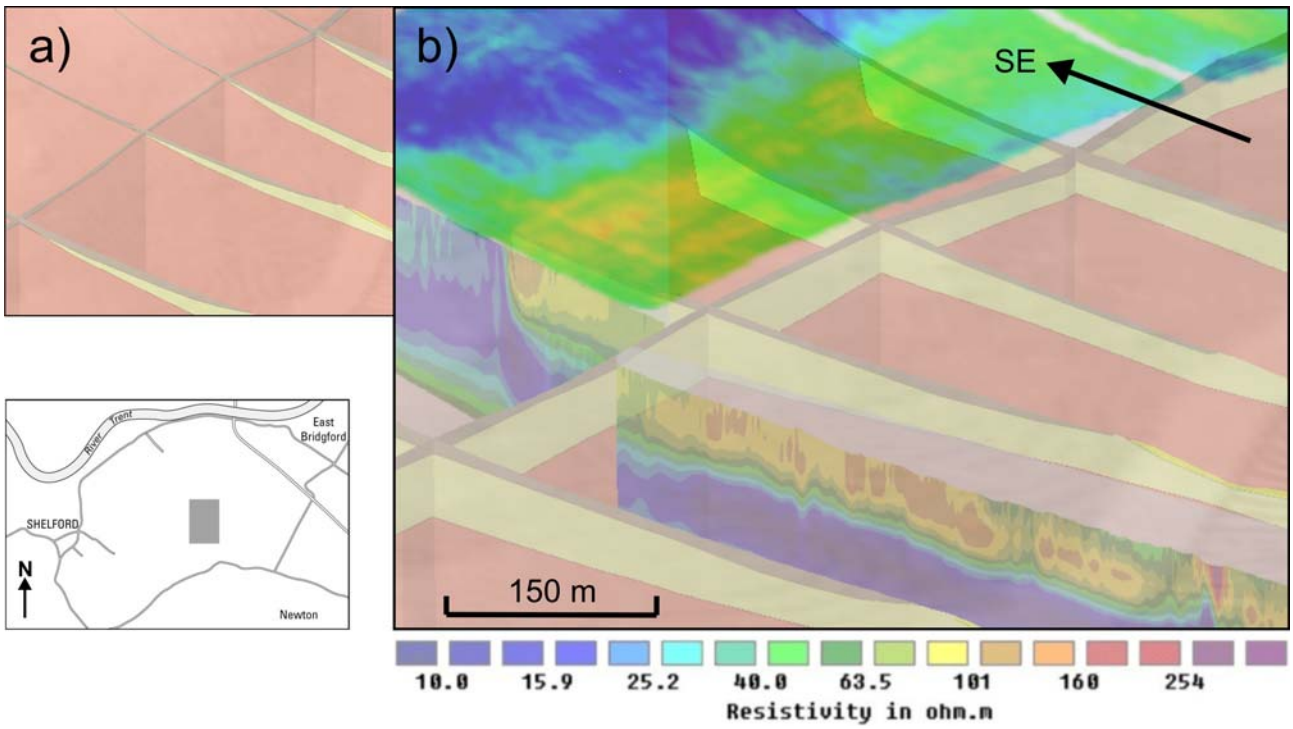
a)
b)
SE
River Trent
East Bridgford
SHELFORD
N
Newton
150 m
10.0
15.9
25.2
40.0
63.5
101
160
254
Resistivity in ohm.m

Figure 6:

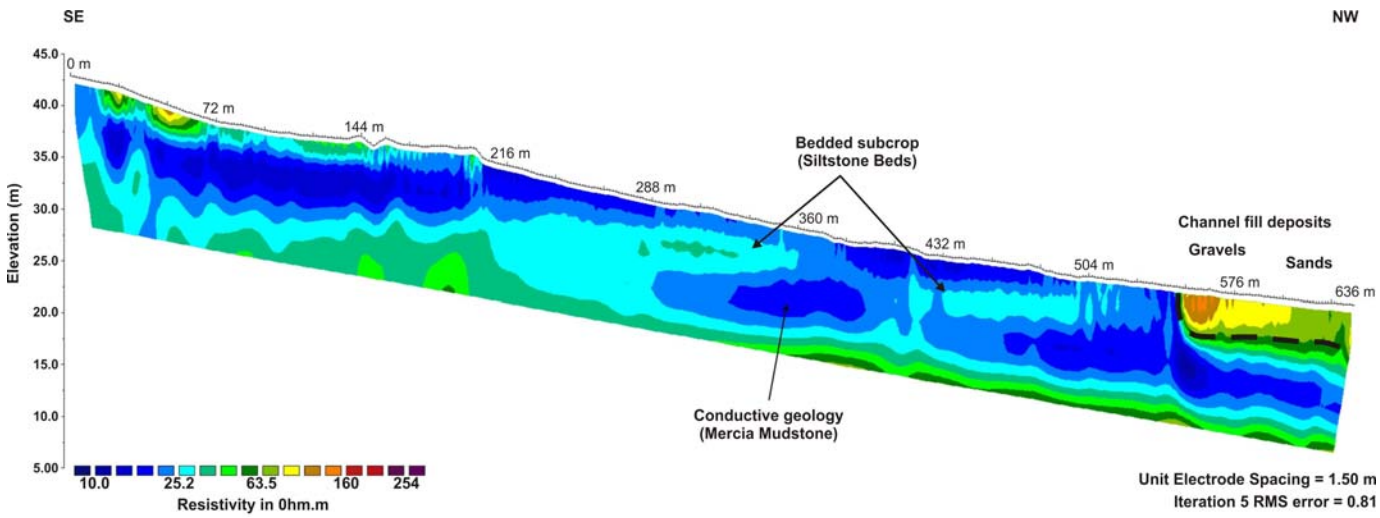
SE
NW
Elevation (m)
45.0
40.0
35.0
30.0
25.0
20.0
15.0
10.0
5.00
0 m
72 m
144 m
216 m
288 m
360 m
432 m
504 m
576 m
636 m
Bedded subcrop
(Siltstone Beds)
Channel fill deposits
Gravels
Sands
Conductive geology
(Mercia Mudstone)
10.0
25.2
63.5
160
254
Resistivity in 0hm.m
Unit Electrode Spacing = 1.50 m
Iteration 5 RMS error = 0.81

Figure 7:

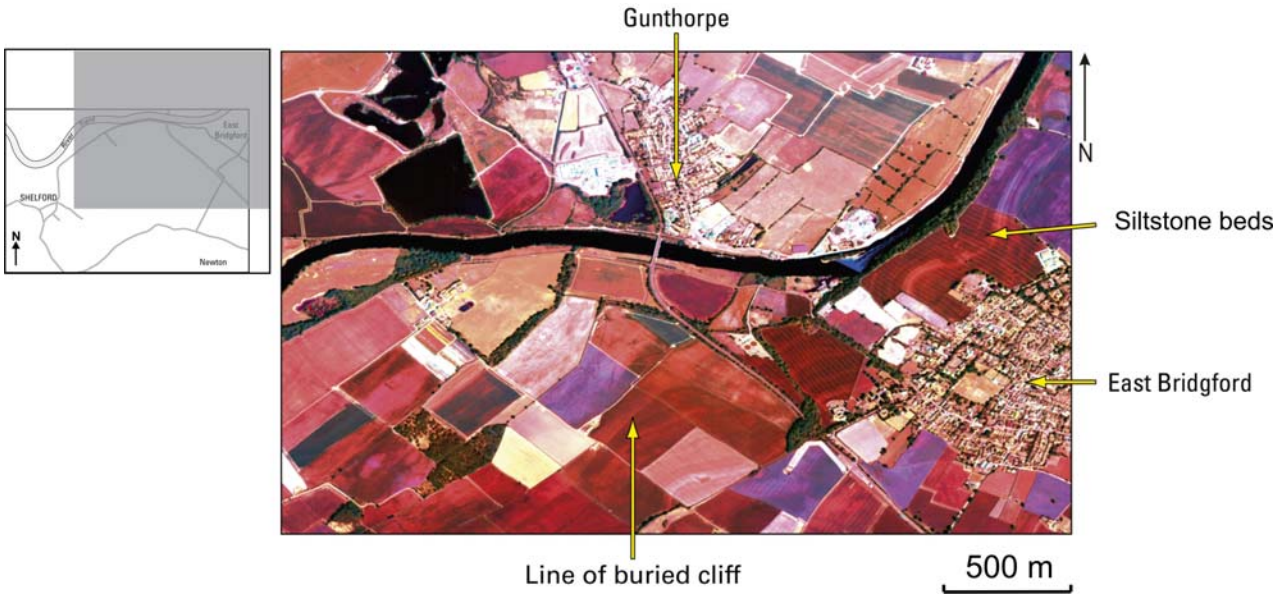
Gunthorpe
SHELFORD
Newton
N
Siltstone beds
East Bridgford
Line of buried cliff
500 m

Figure 8:

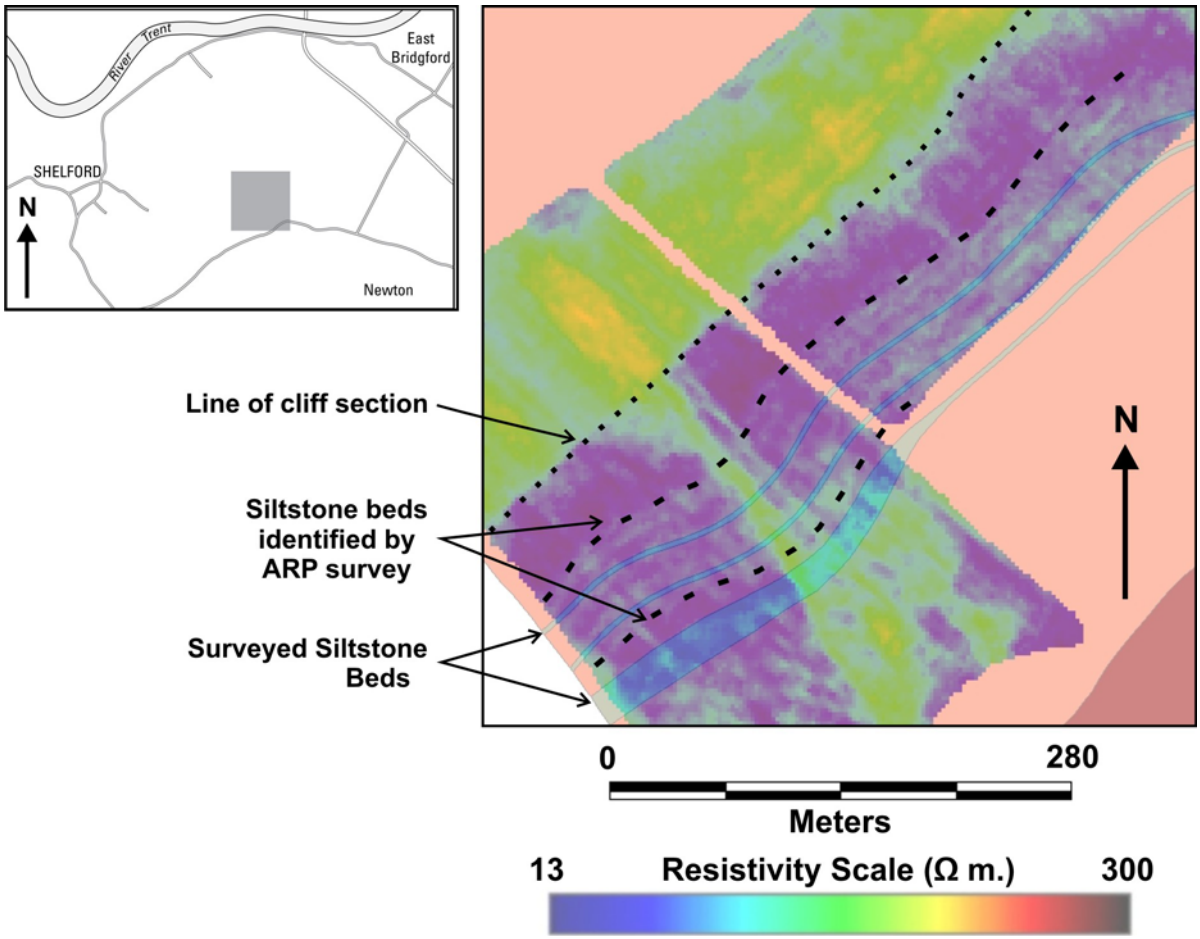
River Trent
East Bridgford
SHELFORD
N
Newton
Line of cliff section
Siltstone beds identified by ARP survey
Surveyed Siltstone Beds
N
0
280
Meters
13
Resistivity Scale (Ω m.)
300

Figure` 9:

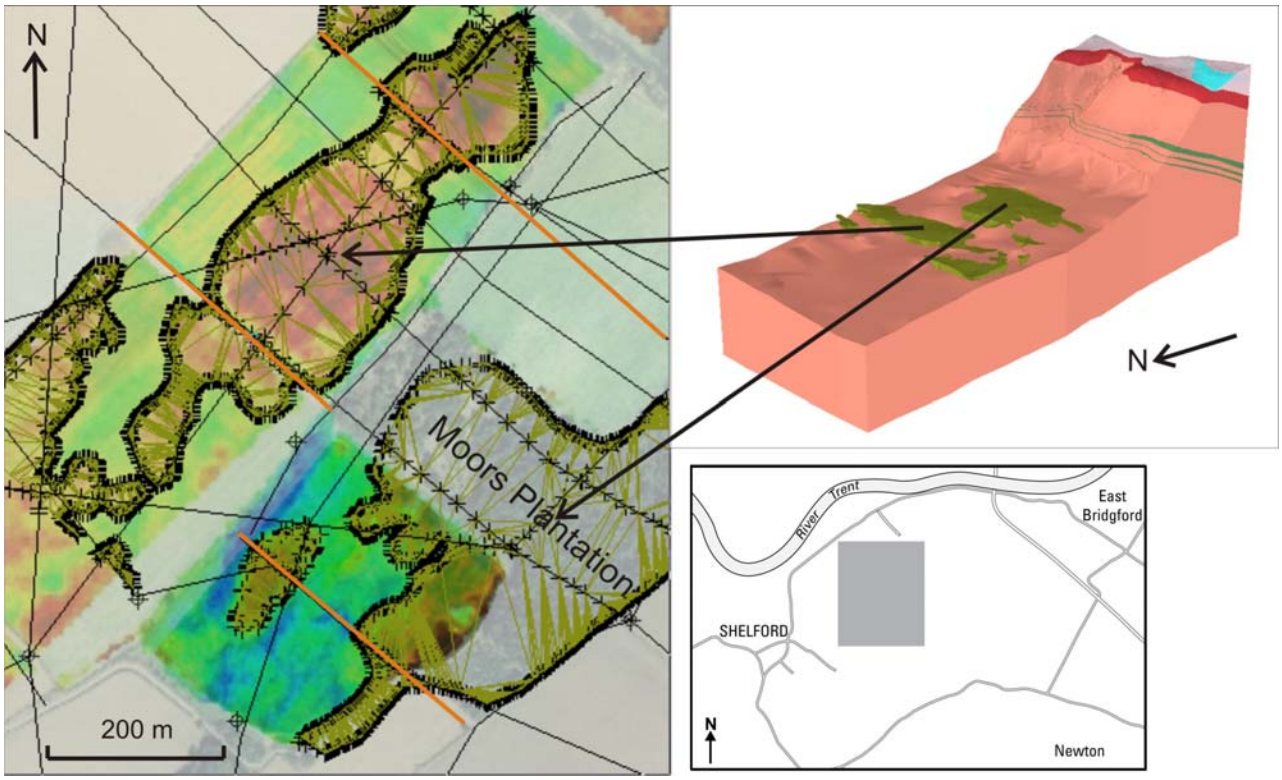
N
Moors Plantation
200 m
N
River Trent
East Bridgford
SHELFORD
Newton
N

Fig 10:

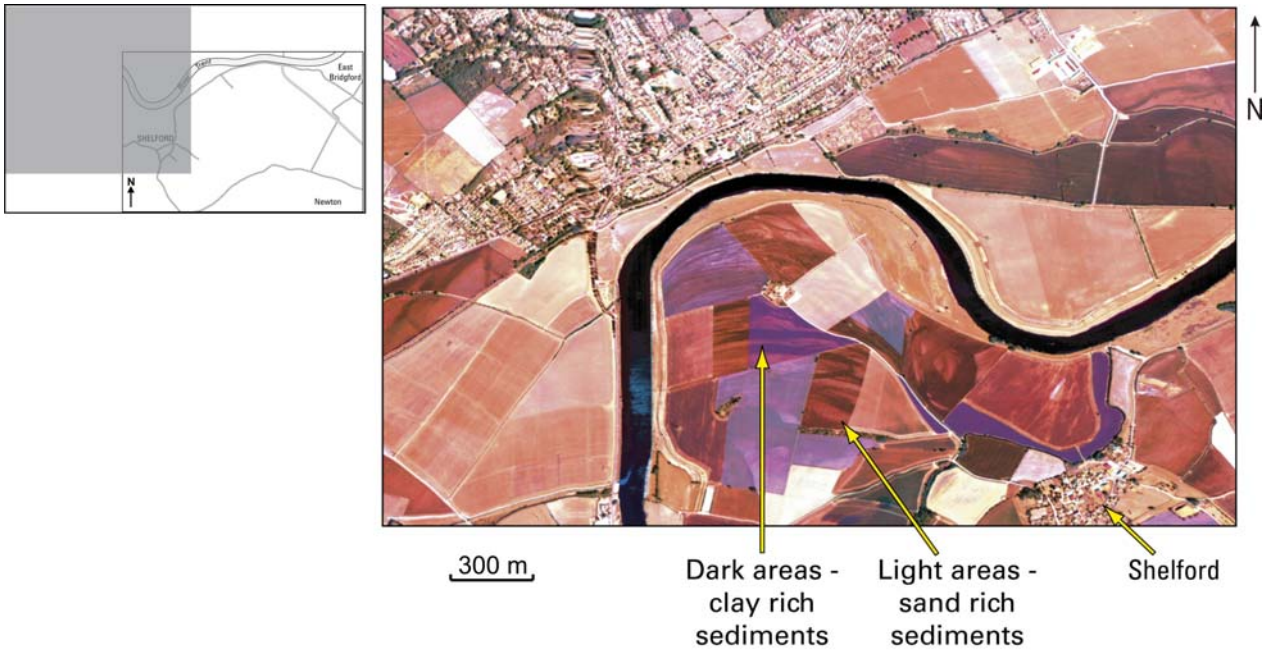
East Bridgford
SHELFORD
Newton
N
N
300 m
Dark areas - clay rich sediments
Light areas - sand rich sediments
Shelford

Figure 11:

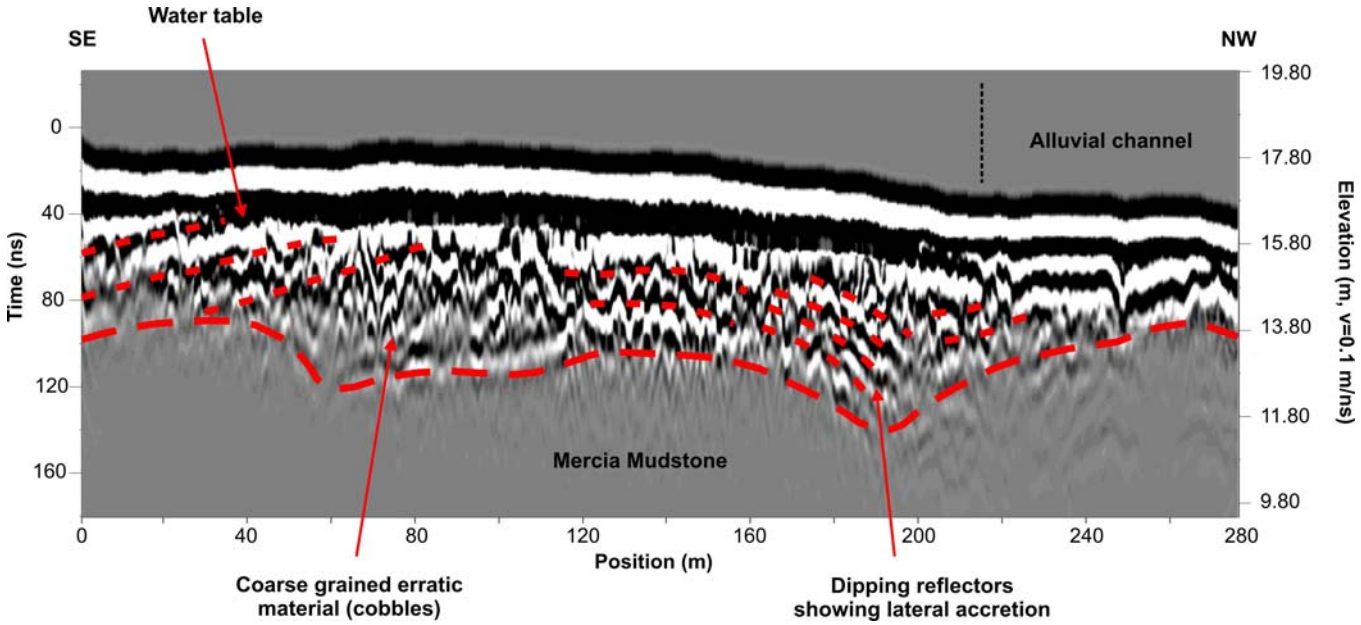
Water table
SE
NW
Alluvial channel
Mercia Mudstone
Time (ns)
0
40
80
120
160
Position (m)
0
40
80
120
160
200
240
280
Elevation (m, v=0.1 m/ns)
19.80
17.80
15.80
13.80
11.80
9.80
Coarse grained erratic material (cobbles)
Dipping reflectors showing lateral accretion

Figure 12:

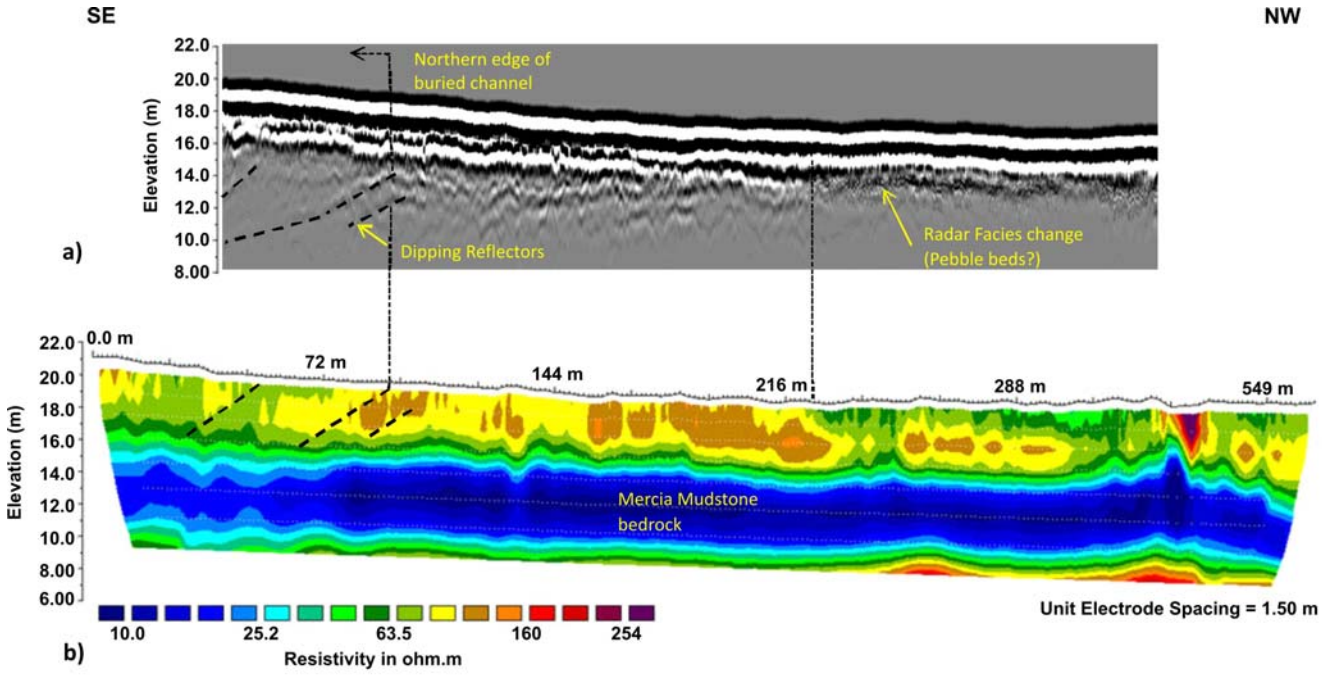
SE
NW
Elevation (m)
22.0
20.0
18.0
16.0
14.0
12.0
10.0
8.00
Northern edge of buried channel
Dipping Reflectors
Radar Facies change (Pebble beds?)
a)
0.0 m
72 m
144 m
216 m
288 m
549 m
Mercia Mudstone bedrock
6.00
10.0
25.2
63.5
160
254
Resistivity in ohm.m
b)
Unit Electrode Spacing = 1.50 m

Figure 13:

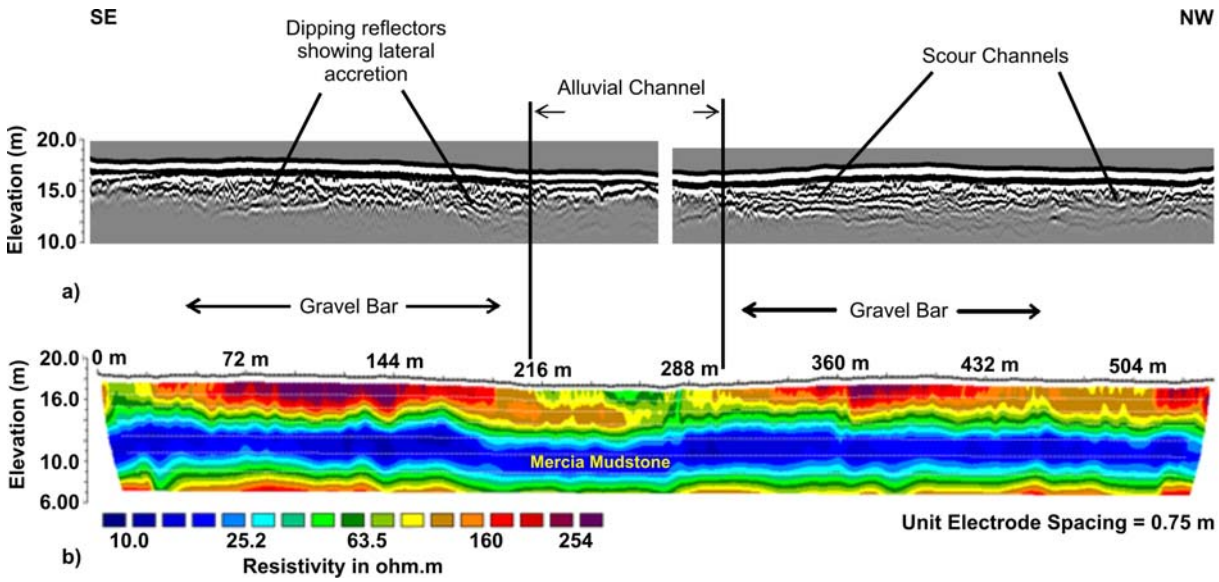
SE
NW
Dipping reflectors showing lateral accretion
Alluvial Channel
Scour Channels
Elevation (m)
20.0
15.0
10.0
a)
Gravel Bar
Gravel Bar
20.0
16.0
10.0
6.00
0 m
72 m
144 m
216 m
288 m
360 m
432 m
504 m
Mercia Mudstone
10.0
25.2
63.5
160
254
b)
Resistivity in ohm.m
Unit Electrode Spacing = 0.75 m

Figure 14:

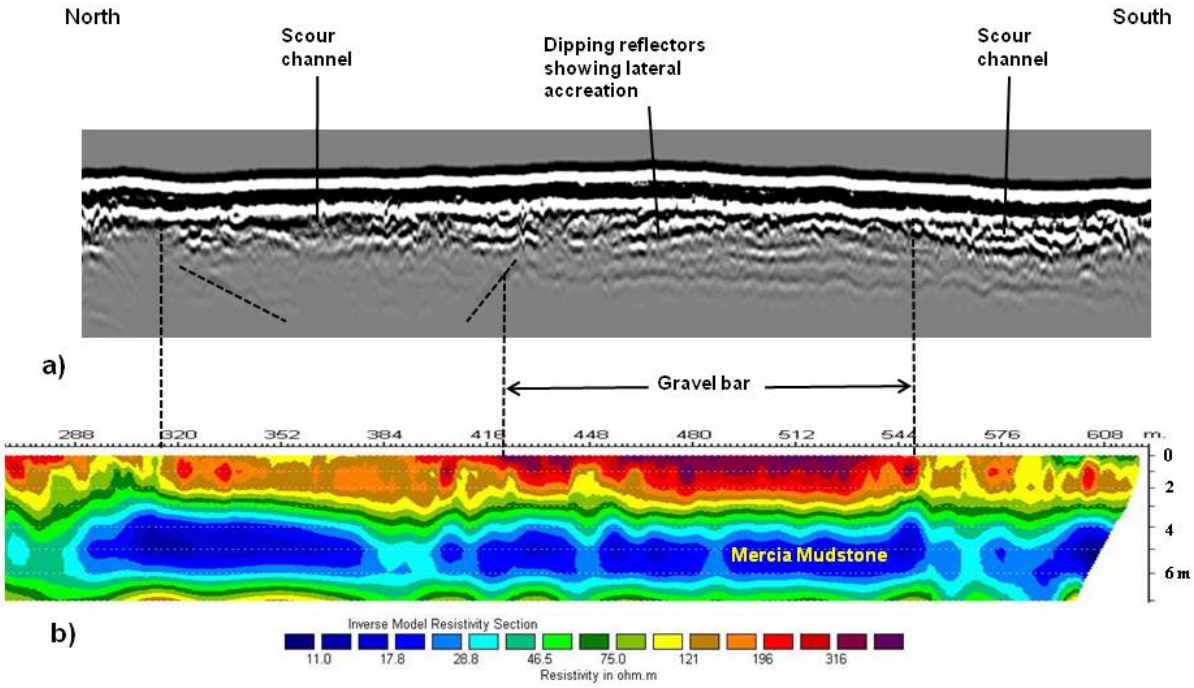
North
South
Scour channel
Dipping reflectors showing lateral accreation
Scour channel
a)
Gravel bar
288
320
352
384
416
448
480
512
544
576
608
m.
0
2
4
6 m
Mercia Mudstone
b)
Inverse Model Resistivity Section
11.0
17.8
28.8
46.5
75.0
121
196
316
Resistivity in ohm.m